

# A Novel Cause of Chronic Viral Meningoencephalitis: Cache Valley Virus

Michael R. Wilson, MD, MAS,<sup>1,2</sup> Dan Suan, MBBS, PhD,<sup>3</sup>  
 Andrew Duggins, MBBS, PhD,<sup>4</sup> Ryan D. Schubert, MD,<sup>1,2</sup> Lillian M. Khan, BS,<sup>5</sup>  
 Hannah A. Sample, BS,<sup>5</sup> Kelsey C. Zorn, MHS,<sup>5</sup>  
 Aline Rodrigues Hoffman, DVM, PhD,<sup>6</sup> Anna Blick, BS,<sup>6</sup>  
 Meena Shingde, FRCPA,<sup>7</sup> and Joseph L. DeRisi, PhD<sup>5,8</sup>

**Objective:** Immunodeficient patients are particularly vulnerable to neuroinvasive infections that can be challenging to diagnose. Metagenomic next generation sequencing can identify unusual or novel microbes and is therefore well suited for investigating the etiology of chronic meningoencephalitis in immunodeficient patients.

**Methods:** We present the case of a 34-year-old man with X-linked agammaglobulinemia from Australia suffering from 3 years of meningoencephalitis that defied an etiologic diagnosis despite extensive conventional testing, including a brain biopsy. Metagenomic next generation sequencing of his cerebrospinal fluid and brain biopsy tissue was performed to identify a causative pathogen.

**Results:** Sequences aligning to multiple Cache Valley virus genes were identified via metagenomic next generation sequencing. Reverse transcription polymerase chain reaction and immunohistochemistry subsequently confirmed the presence of Cache Valley virus in the brain biopsy tissue.

**Interpretation:** Cache Valley virus, a mosquito-borne orthobunyavirus, has only been identified in 3 immunocompetent North American patients with acute neuroinvasive disease. The reported severity ranges from a self-limiting meningitis to a rapidly fatal meningoencephalitis with multiorgan failure. The virus has never been known to cause a chronic systemic or neurologic infection in humans. Cache Valley virus has also never previously been detected on the Australian continent. Our research subject traveled to North and South Carolina and Michigan in the weeks prior to the onset of his illness. This report demonstrates that metagenomic next generation sequencing allows for unbiased pathogen identification, the early detection of emerging viruses as they spread to new locales, and the discovery of novel disease phenotypes.

ANN NEUROL 2017;82:105–114

Outbreaks of emerging and reemerging pathogens have stimulated international discussion about the most efficient means for improving early detection so that public and private resources can be mobilized quickly and efficiently to limit widespread transmission and treat affected patients. There is a growing consensus that an optimal surveillance regimen will (1) incorporate an unbiased approach to pathogen identification and (2)

focus surveillance efforts on groups of people at high risk for unusual infections (eg, immunodeficient patients and people with relevant exposures).<sup>1–3</sup> An unbiased approach to pathogen identification is important because traditional candidate-based diagnostic tests essentially fail to identify novel and unusual pathogens, usually due to perceived rarity or exclusion from clinical consideration based on established geographical distribution. Global

View this article online at [wileyonlinelibrary.com](http://wileyonlinelibrary.com). DOI: 10.1002/ana.24982

Received Mar 31, 2017, and in revised form Jun 15, 2017. Accepted for publication Jun 16, 2017.

Address correspondence to Dr Wilson, UCSF Weill Institute for Neurosciences, Department of Neurology, University of California, San Francisco, 675 Nelson Rising Ln, Campus Box 3206, San Francisco, CA 94158. E-mail: [michael.wilson@ucsf.edu](mailto:michael.wilson@ucsf.edu)

From the <sup>1</sup>Weill Institute for Neurosciences, University of California, San Francisco, San Francisco, CA; <sup>2</sup>Department of Neurology, University of California, San Francisco, San Francisco, CA; <sup>3</sup>Department of Clinical Immunology and Allergy, Westmead Hospital, Westmead, New South Wales, Australia; <sup>4</sup>Department of Neurology, Westmead Hospital, Westmead, New South Wales, Australia; <sup>5</sup>Department of Biochemistry and Biophysics, University of California, San Francisco, San Francisco, CA; <sup>6</sup>Department of Veterinary Pathobiology, College of Veterinary Medicine and Biomedical Sciences, Texas A&M University, College Station, TX; <sup>7</sup>Tissue Pathology and Diagnostic Oncology, Institute of Clinical Pathology and Medical Research, Westmead Hospital, Westmead, New South Wales, Australia; and <sup>8</sup>Chan Zuckerberg Biohub, San Francisco, CA

© 2017 The Authors Annals of Neurology published by Wiley Periodicals, Inc. on behalf of American Neurological Association. 105  
 This is an open access article under the terms of the Creative Commons Attribution NonCommercial License, which permits use, distribution and reproduction in any medium, provided the original work is properly cited and is not used for commercial purposes.

surveillance efforts need to be streamlined, because it is both time-consuming and costly for physicians to order many pathogen-specific tests for geographically and clinically novel organisms. Finally, in the modern era, when international travel has become so commonplace, the need for improved pathogen detection has become clear.

Here, we report the effective deployment of metagenomic next generation sequencing (mNGS) to diagnose Cache Valley virus (CVV), a mosquito-borne orthobunyavirus,<sup>4</sup> in an Australian patient with a primary immunodeficiency suffering from chronic meningoencephalitis. This case demonstrates the power of mNGS to identify the possible movement of an emerging, mosquito-borne virus to a new continent. Only previously associated with acute neuroinvasive disease, this report also extends the phenotype of CVV infection in humans.<sup>5–7</sup>

## Patient and Methods

### Case

The patient is a 34-year-old man from Australia with a history of hypochondroplasia and X-linked agammaglobulinemia (confirmed germline mutations in fibroblast growth factor receptor 3 [*FGFR3*] and Bruton tyrosine kinase [*BTK*], respectively). The antibody deficiency was diagnosed in infancy, and the patient commenced lifelong intravenous immunoglobulin (IVIg) therapy. The patient suffered from chronic sinusitis despite IVIg therapy and was treated with clarithromycin prophylaxis. Despite mild developmental delay and associated learning difficulties, he completed school and vocational training and went on to full-time employment as a retail store manager.

In 2013, the patient traveled to the United States on 3 occasions. The first trip was to Raleigh, North Carolina in the spring. The second visit, in the summer 3 months later, started in Raleigh, but also included a trip to Charleston, South Carolina, where the patient participated in tubing along the local river. It was during this nearly month-long trip that the patient complained of a mosquito bite to his traveling companion. Two weeks later, he traveled to East Lansing, Michigan. Upon returning home to Australia 3 weeks later, the patient fell ill within 2 days, with his parents reporting fatigue, anorexia, and lethargy. Six days later, the patient suffered an acute encephalitic illness characterized by fevers to 39°C, confusion, and postictal drowsiness following 2 generalized tonic-clonic seizures. The patient was intubated and transferred to the intensive care unit. Blood tests revealed lymphocytosis ( $23.3 \times 10^9/l$ , normal range [NR] =  $1.0\text{--}3.0 \times 10^9/l$ ) and a C-reactive protein level of 17.9mg/l (NR  $\leq 5$ mg/l). Cerebrospinal fluid (CSF)

studies revealed normal concentrations of protein (32 mg/dl) and glucose (77 mg/dl), with  $87 \times 10^6/l$  white blood cells (11% neutrophils, 38% lymphocytes, 51% monocytes) and  $19 \times 10^6/l$  red blood cells. Magnetic resonance imaging (MRI) of the brain revealed increased T2 signal and restricted diffusion through the right fornix, extending into the right hippocampus and amygdala (Fig 1A, B) with interval development of contrast enhancement in the same brain structures 2 weeks later (Fig 1C, D). Microbiological tests, including culture and polymerase chain reaction (PCR) for candidate pathogens, failed to identify an organism (Tables 1 and 2). The patient was treated empirically with acyclovir, ceftriaxone, benzylpenicillin, and vancomycin. Vancomycin and benzylpenicillin were discontinued due to the development of a rash on the patient's hip, and azithromycin was started due to left-sided consolidation observed on his chest x-ray. The patient completed 10 days of antimicrobial therapy with clinical improvement, and his seizure disorder was controlled with levetiracetam and sodium valproate. He was discharged from the hospital, but was readmitted 4 days later with hypersomnolence and a fluctuating level of consciousness. His antiepileptic medications were adjusted, and he was discharged home again. The patient made a partial recovery over the next 2 months but had new short-term memory loss. He was ultimately able to return to work in a reduced capacity. Over the next 2 years, the patient remained seizure free. He utilized compensatory coping strategies at work due to the significant short-term memory deficit, but he was otherwise independent with activities of daily living at home with his parents. There were reports of anxiety and fatigue, but no specific diagnoses were made.

In the spring of 2016, the patient presented for reevaluation. His parents reported 6 months of progressive memory decline, slowing of speech, mood disturbance (predominantly anxiety), and intermittent tremors. He was no longer able to work due to his encephalopathy and needed assistance with activities of daily living. Neurologic examination revealed that language was fluent but monotonous. His Montreal Cognitive Assessment score was 7/30 with severe impairment in visuospatial and executive function, attention, abstraction, and delayed recall.<sup>8</sup> He could not perform the Luria maneuver and was unable to mimic simple hand gestures. He had a fine, jerky, postural tremor with his arms outstretched. He had diffuse muscle rigidity with 6 beats of ankle clonus bilaterally. He could stand independently but had a broad-based gait with reduced stride length, stooped posture, and en bloc turning. A follow-up brain MRI demonstrated interval development of diffuse cerebral atrophy with ex vacuo hydrocephalus and additional

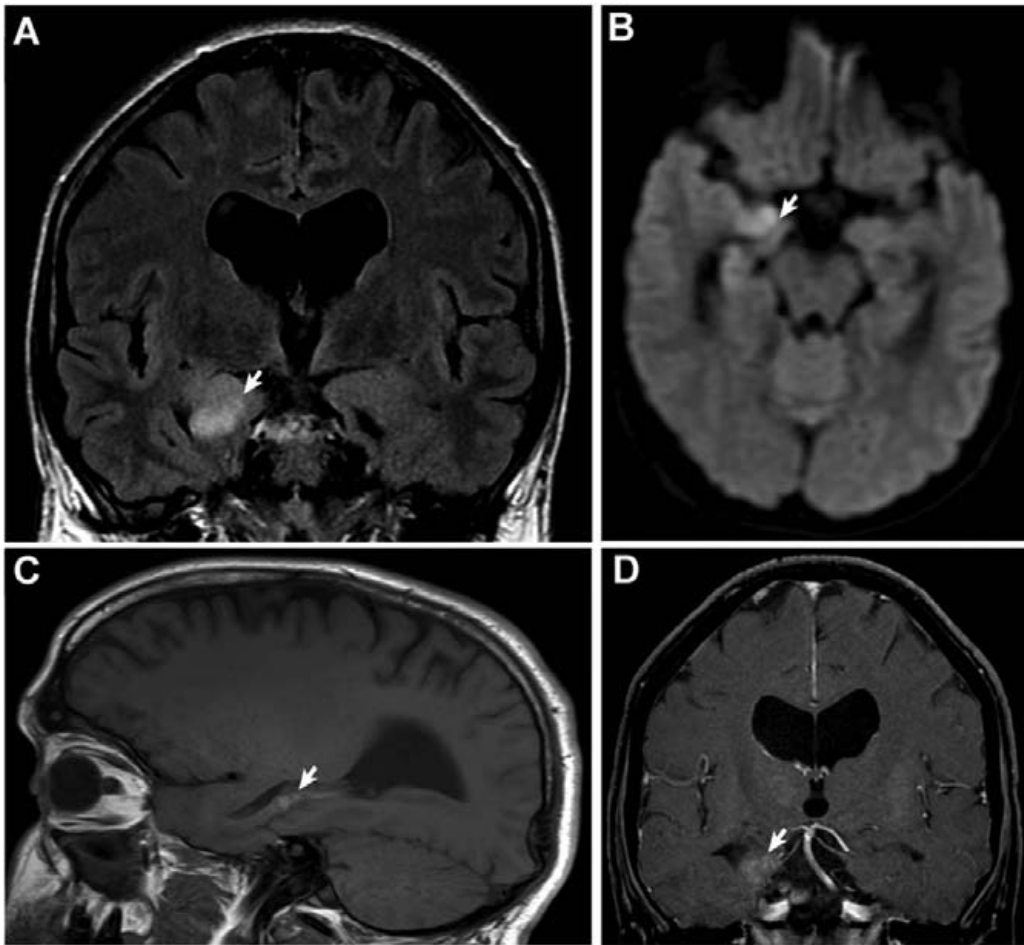


**FIGURE 1:** Neuroimaging from acute presentation. (A) Coronal T2-weighted/fluid-attenuated inversion recovery brain magnetic resonance imaging (MRI) demonstrating T2 hyperintensity in the right hippocampus and amygdala (arrow). (B) Axial diffusion-weighted imaging brain MRI demonstrating restricted diffusion in the right hippocampus and amygdala (arrow). (C, D) Sagittal (C) and coronal (D) T1-weighted postcontrast brain MRI demonstrating contrast enhancement 2 weeks after the acute presentation (arrows).

focal atrophy of the right medial temporal lobe (Fig 2C and D). An MRI of the spinal cord was unremarkable. Repeat CSF examination was unremarkable (Table 2) and showed a normal opening pressure. Normal pressure hydrocephalus was excluded by large volume CSF extraction (30 ml) and comparative neuropsychological testing.

A brain biopsy of the right frontal lobe revealed features of meningoencephalitis, with inflamed fibrous leptomeninges, scattered microglial nodules, and a perivascular as well as interstitial lymphocytic infiltrate in the cortex (Fig 3). The white matter also contained a few microglial nodules and small number of perivascular lymphocytes (not shown). The perivascular and interstitial lymphocytic infiltrate was composed predominantly of CD8<sup>+</sup> T lymphocytes. No viral cytopathic changes were seen. Conventional CSF and brain biopsy studies failed to identify a causative organism (Table 2).

### Sequencing Library Preparation

A 250  $\mu$ l sample of CSF and a <50mg piece of surplus brain biopsy tissue were collected in RNase/DNase-free Lobind tubes (Sigma-Aldrich, St Louis, MO) and snap frozen in liquid nitrogen. The samples were submitted for unbiased mNGS under a research protocol (#13-12236) for the identification of potential pathogens approved by the institutional review board of the University of California, San Francisco (UCSF). A common issue in metagenomic sequencing is that essentially all reagents used during the library preparation process contain some extraneous nucleic acid, including material commonly present in laboratory reagents.<sup>9,10</sup> The process of acquiring a human sample can also introduce unwanted nucleic acid from skin or environmental contamination. To control for irrelevant sequences, an unrelated, uninfected human CSF sample ("control") was prepared in parallel and sequenced on the same run in addition to a water control. Samples were processed for

TABLE 1. Peripheral Clinical Laboratory Results

Test	Site	Initial Presentation, 2013	Follow-Up Evaluation, 2016
C-reactive protein	Blood	17.9mg/l ( $\leq 5.0$ )	$< 5$ ( $\leq 5.0$ )
Immunoglobulin A	Blood	$< 0.07$ g/l (0.70–3.12)	
Immunoglobulin G	Blood	8.24g/l (6.39–15.60)	11.8 (6.6–15.6)
Immunoglobulin M	Blood	$< 0.20$ g/l (0.50–3.00)	
Legionella Ag	Urine	Negative	
Pneumococcal Ag	Urine	Negative	
Respiratory multiplex DNA/RNA	Nasal swab	Enterovirus detected	
Bacterial culture	Blood	3 cultures: negative	5 cultures: negative
Bacterial culture	Sputum	Negative	Beta lactamase positive, <i>Haemophilus influenzae</i>
Bacterial culture	Nasal swab	Negative	
Fungal culture	Blood	Negative	
Chlamydia CFT	Blood	Negative	
<i>Legionella pneumophila</i> (1–8) IFA titer	Blood	$< 128$	
<i>Legionella longbeachae</i> IFA titer	Blood	$< 128$	
Lyme EIA	Blood	Not detected	
Lyme borrelia Ab	Blood	Negative	
<i>Mycoplasma pneumoniae</i> IgM	Blood	Negative	
AST	Blood	41U/l (5–55)	18U/l ( $\leq 40$ )
ALT	Blood	52U/l (5–55)	20U/l ( $\leq 40$ )
Alkaline phosphatase	Blood	114IU/l (30–130)	114IU/l (30–110)
Protein	Blood	64g/l (62–80)	78g/l (60–80)
GGT	Blood	52U/l ( $\leq 60$ )	13U/l ( $\leq 50$ )
WBC	Blood	$23.3 \times 10^9$ /l (4.0–10.0)	$5.9 \times 10^9$ /l (3.7–9.5)
Neutrophils	Blood	$12.8 \times 10^9$ /l (2.0–7.0)	$2.8 \times 10^9$ /l (2.0–8.0)
Lymphocytes	Blood	$8.6 \times 10^9$ /l (1.0–3.0)	$2.0 \times 10^9$ /l (1.0–4.0)
Monocytes	Blood	$0.9 \times 10^9$ /l (0.2–1.0)	$1.0 \times 10^9$ /l (0.2–1.0)
Eosinophils	Blood	0 (0–0.5)	$0.1 \times 10^9$ /l (0.0–0.5)
Reactive lymphocytes	Blood	Present	
Band forms	Blood	$0.9 \times 10^9$ /l	
Hemoglobin	Blood	152g/l (130–170)	147g/l (130–180)
Platelets	Blood	$427 \times 10^9$ /l (150–450)	$301 \times 10^9$ /l (140–400)

Ab = antibody; Ag = antigen; ALT = alanine aminotransferase; AST = aspartate aminotransferase; CFT = complement fixation test; EIA = enzyme-linked immunosorbent assay; GGT = gamma-glutamyl transferase; IFA = indirect fluorescent antibody; IgM = immunoglobulin M; WBC = white blood cell count.

mNGS analysis as previously described.<sup>11–13</sup> Briefly, total RNA was extracted. The sequencing library was prepared with New England Biolabs' (NEB; Ipswich, MA)

NEBNext RNA First Strand Synthesis Module (E7525) and NEBNext Ultra Directional RNA Second Strand Synthesis Module (E7550) to generate double-stranded

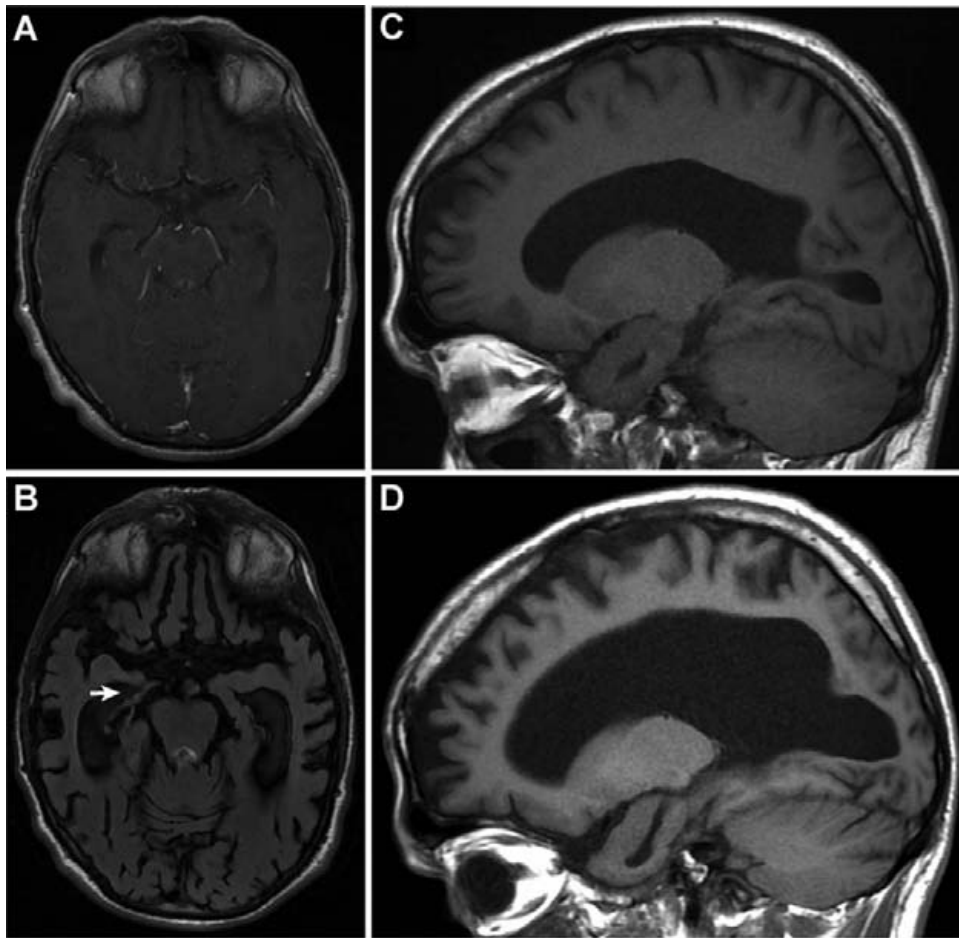


**FIGURE 2:** Neuroimaging at 3-year follow-up. (A, B) Axial T1-weighted brain magnetic resonance imaging (MRI) at the acute presentation (A) and at 3-year follow-up (B) with interval development of severe, diffuse cerebral atrophy, ex vacuo hydrocephalus, and focal atrophy of the right hippocampus (arrow). (C, D) Sagittal T1-weighted brain MRIs at the acute presentation (C) and at 3-year follow-up (D) with interval development of severe, diffuse cerebral atrophy, and ex vacuo hydrocephalus.

complementary DNA (cDNA). The cDNA was converted to Illumina (San Diego, CA) libraries using the NEBNext Ultra II DNA library preparation kit (E7645) according to the manufacturer's recommendation and amplified with 11 PCR cycles. The libraries were subjected to an additional step to selectively deplete library amplicons whose sequences corresponded to the human mitochondrial genome. This was accomplished via Depletion of Abundant Sequences by Hybridization (DASH), a novel molecular technique using the CRISPR (Clustered Regularly Interspaced Short Palindromic Repeats)-associated nuclease Cas9 in vitro.<sup>11,13</sup> The pooled library was size-selected using Ampure beads, and concentration was determined using a Kapa Universal quantitative PCR kit (Kapa Biosystems, Woburn, MA). Samples were sequenced on an Illumina HiSeq 4000 instrument using 140/140 base pair paired-end sequencing.

### **Bioinformatics**

Sequences were analyzed using a rapid computational pipeline developed by the DeRisi Laboratory to classify

mNGS reads and identify potential pathogens by comparison to the entire National Center for Biotechnology Information (NCBI) nucleotide (nt) reference database, which has previously been described in detail.<sup>11,13</sup> Briefly, all paired-end reads were aligned to the human reference genome 38 (hg38) and the *Pan troglodytes* genome (pan-Tro4; 2011, University of California, Santa Cruz).<sup>14</sup> Unaligned (ie, nonhuman) reads were quality filtered using PriceSeqFilter.<sup>15</sup> Quality filtered reads were then compressed by cd-hit-dup (v4.6.1), and low-complexity reads were removed via the Lempel-Ziv-Welch algorithm.<sup>16,17</sup> Next, human removal was repeated using Bowtie2 (v2.2.4) with the same hg38 and PanTro4 reference genomes as described above.<sup>18</sup> GSNAPL (v2015-12-31)<sup>19</sup> was used to align the remaining nonhuman read pairs to the NCBI nt database and preprocessed to remove known repetitive sequences with RepeatMasker (vOpen-4.0; www.repeatmasker.org). The same reads were also aligned to the NCBI nonredundant protein (nr) database using the Rapsearch2 algorithm.<sup>20</sup> The resulting sequence hits identified at both the nt and

**TABLE 2. Central Nervous System Clinical Laboratory Results**

Test	Site	Initial Presentation, 2013	Follow-up Evaluation, 2016
RBC	CSF	19 cells/mm <sup>3</sup>	18 cells/mm <sup>3</sup>
WBC	CSF	87 cells/mm <sup>3</sup>	4 cells/mm <sup>3</sup>
Neutrophils	CSF	11%	0
Lymphocytes	CSF	38%	100%
Monocytes	CSF	51%	0
Protein	CSF	32mg/dl	37mg/dl (40–70)
Glucose	CSF	77mg/dl	52mg/dl (15–50)
Lactate	CSF	2.0mmol/l (1.2–2.8)	1.96mmol/l (1.0–2.9)
Gram stain	CSF	Negative	Negative
AFB stain	CSF		Negative
Fungal culture	CSF		Negative
Bacterial culture	CSF	Negative	Negative
Mycobacterial culture	CSF		Negative
<i>Borrelia burgdorferi</i> culture	CSF		Negative
Cytomegalovirus DNA	CSF	Negative	Negative
Enterovirus RNA	CSF	Negative	Negative
HSV-1, 2 DNA	CSF	Negative	Negative
VZV DNA	CSF	Negative	Negative
<i>Neisseria meningitidis</i> DNA	CSF	Negative	
16S rRNA	CSF		Negative
Enterovirus RNA	CSF		Negative
HHV-6 DNA	CSF		Negative
Polyomavirus DNA	CSF		Negative
<i>Toxoplasma gondii</i> DNA	CSF		Negative
VZV DNA	CSF		Negative
EBV quantitation DNA	CSF		Negative
Parechovirus RNA	CSF		Negative
Cryptococcal Ag	CSF	Negative	
Giemsa stain	Brain		Negative
PAS stain	Brain		Negative
Ziehl–Neelsen stain	Brain		Negative
Methenamine silver stain	Brain		Negative
Warthin–Starry stain	Brain		Negative
Fungal culture	Brain		Negative
Bacterial culture	Brain		Negative
Mycobacterial culture	Brain		Negative
Cytomegalovirus DNA	Brain		Negative
Bacterial DNA, 16S rRNA NAT	Brain		Negative
Enterovirus RNA	Brain		Negative
HHV-6 DNA	Brain		Negative
HSV-1, 2 DNA	Brain		Negative
Polyomavirus DNA	Brain		Negative
<i>Toxoplasma gondii</i> DNA	Brain		Negative
VZV DNA	Brain		Negative
EBV DNA	Brain		Negative
Parechovirus RNA	Brain		Negative
HHV-8 DNA	Brain		Negative

AFB = acid-fast bacilli; Ag = antigen; CSF = cerebrospinal fluid; EBV = Epstein–Barr virus; HHV = human herpes virus; HSV = herpes simplex virus; 16S rRNA = 16S ribosomal RNA; NAT = nucleic acid amplification test; PAS = periodic acid–Schiff; RBC = red blood cell count; VZV = varicella zoster virus; WBC = white blood cell count.

protein (translated) level from the control patient and water samples were subtracted from each patient sample by matching genus or species level taxonomic identifications (taxids). Organisms were further investigated if they were present at  $>0.2$  nonredundant, mapped read pairs per million read pairs at the species level based on nt alignment (1 read per 5 million nonredundant reads).

## Results

### Sequencing Results

A total of 25,069,677 and 13,661,871 paired-end reads were obtained from the CSF and brain biopsy specimens, respectively. As described above, the paired-end sequences were processed through a custom bioinformatics pipeline. The runtime for the bioinformatics pipeline described above was 10 to 15 minutes per sample on a single 24-core server. After filtering, there were 2 genera remaining in the mNGS dataset from the CSF sample: Bunyamwera virus (taxid: 35304) and cucumber green mottle mosaic virus (taxid: 12234). Only Bunyamwera virus was considered a credible pathogen. At the species level, the 5 unique pairs of Bunyamwera virus reads mapped to the CVV nucleoprotein and RNA-dependent RNA polymerase with 89 to 100% similarity. Although no Bunyamwera virus sequences were identified in the nt results from the brain biopsy sample, the nr output identified 2 unique read pairs that mapped with 99 to 100% similarity to the CVV S (small) genome segment that encodes the nucleocapsid protein and a nonstructural

protein. Thus, the very simple and conservative algorithm described above resulted in a single taxonomic category (CVV) in our patient's CSF sample, which, upon further investigation, was also present in the brain biopsy sample. CVV is an orthobunyavirus known to cause acute neuroinvasive disease but not a chronic meningoencephalitis. CVV sequences have never been previously detected in this laboratory, nor have CVV reagents or materials been present in this laboratory. These nonhuman sequence reads corresponding to the libraries from this patient have been deposited at the NCBI Sequence Read Archive BioProject (PRJNA338853).

### Confirmatory Testing

Reverse transcription-PCR (RT-PCR) was performed on the patient's brain biopsy tissue and CSF using previously published CVV primers for the polyprotein gene (ie, CVV forward [CCAATGCAATTCAGGGCAGT] and reverse [TGAGTCACCACATGCTGTAAGGT]) according to a slightly modified version of a published protocol.<sup>21</sup> RT-PCR was unsuccessful from CSF, but the amplicon from the brain biopsy tissue RNA was cloned into One Shot TOP10 chemically competent *Escherichia coli* using the TOPO-TA cloning kit according to the manufacturer's protocol (Thermo Fisher Scientific, Waltham, MA). Ampicillin-resistant colonies were Sanger sequenced (Quintara Biosciences, South San Francisco, CA). The cloned sequence unambiguously aligned to CVV (98% similarity); a Basic Local Alignment Search Tool search of NCBI also returned only CVV hits and

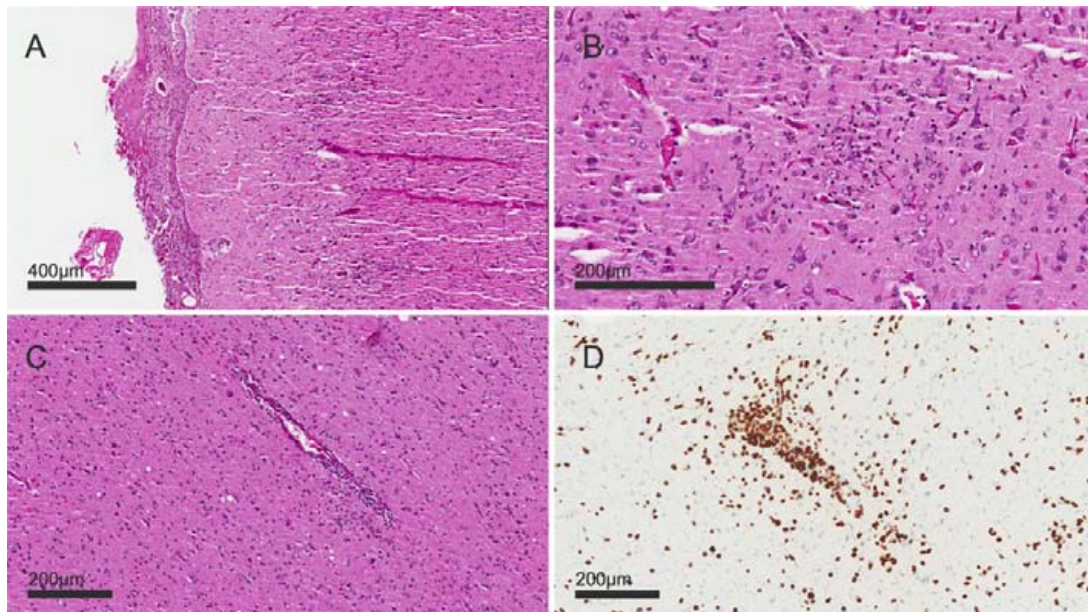


**FIGURE 3: Neuropathology.** (A) Leptomeningeal thickening and inflammation. (B) Microglial nodule in the cortex. (C) Perivascular and interstitial lymphocytic infiltrate in the cortex. (D) Perivascular and interstitial lymphocytic infiltrates of predominantly CD8<sup>+</sup> T lymphocytes visualized by means of immunolabeling with anti-CD8 antibody.

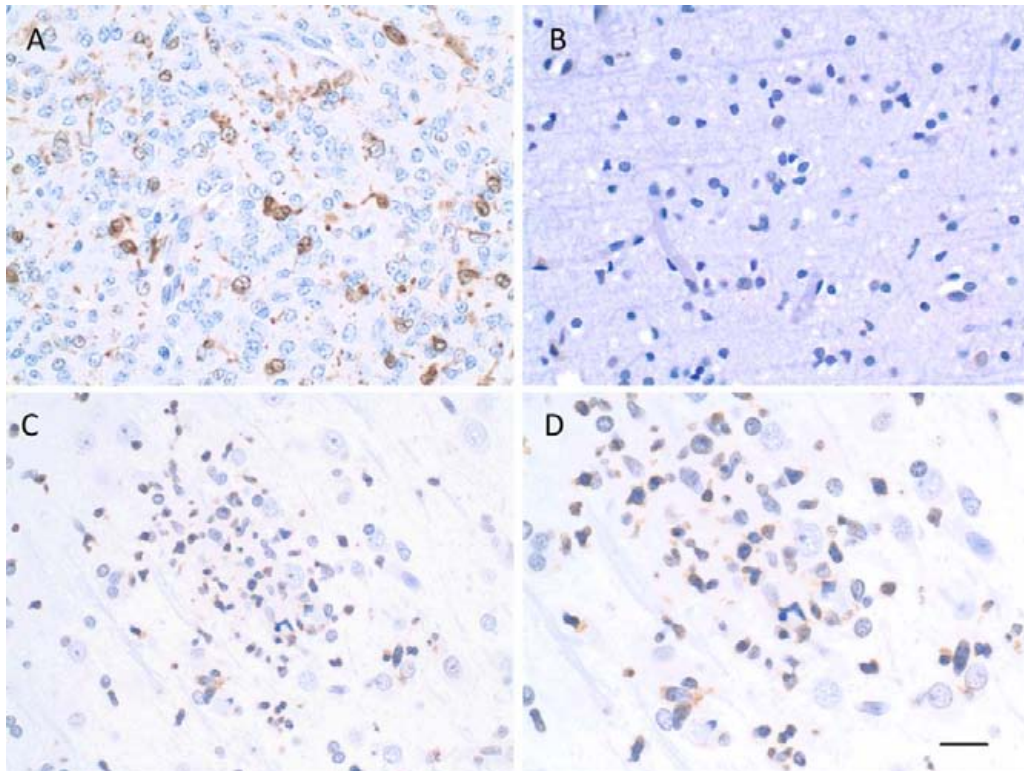


**FIGURE 4: Immunohistochemistry.** (A) Strong intracytoplasmic immunostaining in ovine fetal brain using anti-Cache Valley virus (CVV) polyclonal antibody (Ab) and stained with brown 3,3'-diaminobenzidine chromogen (positive control). (B) No immunostaining in noninfected human brain using anti-CVV polyclonal Ab (negative control). (C, D) Intracytoplasmic immunostaining in subject's brain using anti-CVV polyclonal Ab. Scale bar = 20  $\mu\text{m}$  (A–C) and 13  $\mu\text{m}$  (D).

did not align to any other viruses. The RNA-dependent RNA polymerase sequence of the most closely related Australian orthobunyavirus, Kowanyama virus (GenBank KC436108.1), had only 80% similarity to the viral polymerase sequences obtained from our subject's sample.<sup>22</sup> Virus culture with fresh CSF was attempted on multiple cell lines (Vero, Vero E6, *Aedes albopictus* [C6/36], buffalo green monkey kidney, human fetal lung [MRC-5], and rhabdomyosarcoma [RD]) without success. Immunohistochemistry was performed on 5  $\mu\text{m}$  sections of formalin-fixed, paraffin-embedded tissues following previously described methods with minor modifications, including a rabbit polyclonal antibody against CVV at 1:100 dilution or normal rabbit IgG incubation for 1 hour, a serum-free protein block incubation (Dako, Carpinteria, CA), and a polymer-based secondary antibody incubation (Thermo Fisher Scientific, Fremont, CA).<sup>23</sup> Ovine fetal central nervous system (CNS) tissue and skeletal muscle experimentally infected with CVV and noninfected human brain tissue were included as positive and negative controls, respectively. The experimentally infected ovine fetus demonstrated strong intracytoplasmic immunostaining. No immunostaining was observed in the noninfected human negative control brain tissue. The subject's brain showed intracytoplasmic immunostaining,

primarily seen within glial cells forming glial nodules in the brain parenchyma (Fig 4).

## Discussion

Although viruses are typically associated with acute presentations of meningoencephalitis, some are known to cause chronic CNS infection. Immunocompetent patients have been known to suffer from chronic CNS infections caused by paramyxoviruses such as measles virus, Nipah virus, and herpes viruses such as varicella zoster virus,<sup>24–26</sup> whereas immunodeficient patients can suffer from chronic neurologic infections with human immunodeficiency virus type 1, Epstein–Barr virus, enteroviruses, polyomaviruses, astroviruses, coronavirus, and even mumps virus.<sup>24,27–32</sup>

In this report, we expand the spectrum of viral causes of chronic meningoencephalitis in the setting of immunodeficiency to include the orthobunyavirus CVV, a mosquito-borne orthobunyavirus first identified in Cache Valley, Utah in 1956.<sup>4</sup> Orthobunyaviruses are segmented negative-stranded RNA viruses whose genomes are composed of large, medium, and small segments. Other viruses in the orthobunyavirus family of public health importance include California encephalitis virus, Jamestown Canyon virus, and LaCrosse virus.<sup>33,34</sup> CVV

has rarely been reported to cause neuroinvasive disease in immunocompetent patients, with clinical presentations ranging from a self-limited aseptic meningitis to a fatal meningoencephalitis with multiorgan failure.<sup>5-7</sup> CVV has not previously been reported to cause a chronic infection in humans.

Although there are no approved antiviral agents known to treat CVV, the identification of the virus did reinforce a switch from obtaining IVIg pooled from Australian donors to IVIg pooled from donors in the United States, given the possibility that the latter IVIg donor pool might contain neutralizing antibodies against CVV.<sup>35-37</sup> Unfortunately, this change in treatment strategy did not arrest the patient's relentless neurologic decline. His ataxia progressed until he could no longer walk; he ceased communicating verbally and eventually stopped eating and drifted into a coma. He was placed in hospice care and died in early 2017, 42 months after his initial presentation. After his death, his parents reported that they derived great comfort knowing the underlying cause of their son's illness. Our patient's case highlights the need to make specific microbiological diagnoses both so that targeted therapies can be developed and also to provide clarity to patients and families.

Whereas CVV is widespread throughout North and South America, it and other members of the Bunyamwera serogroup have not been previously detected in Australia.<sup>22</sup> Given that CVV is a mosquito-borne virus that can be carried by at least 33 species of mosquitoes across 7 genera, there are likely mosquito species competent to transmit CVV in Australia.<sup>38,39</sup> Although we have no evidence that wider transmission has occurred, it is plausible that our subject could have transmitted CVV to mosquitos in Australia during the 3-year period since his return from the United States. The possibility of having introduced a mosquito-borne virus to a new locale is made even more salient by the recent international Zika virus crisis. The spread of Zika to Latin America was in part exacerbated by the delayed recognition of its introduction to Brazil. Recent phylogenetic studies have indicated that Zika virus was circulating for 18 months before it was identified as a pathogen, and for 24 months before it was determined that Zika was likely responsible for the recent increase in the incidence of microcephaly.<sup>40</sup> The most dramatic example of a virus spreading undetected among human populations over many decades remains HIV-1.<sup>41</sup>

Because CVV is rarely identified as a cause of human disease and has not been reported in Australia previously, there are no traditional candidate-based diagnostic tests for this virus available in Australia. This unusual case highlights the ability for mNGS to identify pathogens not previously associated with a clinical phenotype and not

known to circulate in a geographic area.<sup>2,3</sup> It is also important to note that mNGS was able to identify CVV in the CSF of this patient; if these results had been available before the brain biopsy, they could have obviated the need for this invasive procedure. The ability to identify unanticipated infections in CSF via mNGS in this patient and others motivates the ongoing prospective, multicenter study currently underway to determine the performance characteristics of an mNGS CSF assay performed in a clinical laboratory environment for patients with acute meningitis with or without encephalitis (<http://www.ciampm.org/project/precision-diagnosis-acute-infectious-diseases>). When applied more broadly to global pathogen surveillance efforts, mNGS will significantly enhance the detection and monitoring of global biothreats. Finally, this case extends the spectrum of viruses known to cause chronic meningoencephalitis.

---

## Acknowledgment

Research reported in this article was supported by the UCSF Center for Next-Gen Precision Diagnostics supported by the Sandler Foundation and William K. Bowes, Jr. Foundation (J.L.D., M.R.W., H.A.S., K.C.Z., L.M.K.); Chan Zuckerberg Biohub (J.L.D.); NIH National Center for Advancing Translational Sciences (award number KL2TR000143, M.R.W.); and NIH National Institutes for Neurological Disorders and Stroke (award number K08NS096117, M.R.W.). Its contents are solely the responsibility of the authors and do not necessarily represent the official views of the NIH.

We thank E. Chow and D. Bogdanoff of the UCSF Center for Advanced Technology for their expertise and assistance operating the Illumina sequencer; K. Knopp for her attempts at virus culture; E. Caverzasi for helping select MRI images for the article; the Sandler and William K. Bowes, Jr. Foundations for their generous philanthropic support; and the patient and his family for their participation in this research program.

## Author Contributions

J.L.D., M.R.W., A.D., and D.S. contributed to the conception and design of the study. All authors contributed to the acquisition and analysis of data. M.R.W., J.L.D., A.D., and D.S. drafted the text. M.R.W., J.L.D., D.S., M.S., and A.R.H. prepared the figures. M.R.W. and D.S. contributed equally to the article.

## Potential Conflicts of Interest

M.R.W. and J.L.D. have a patent pending for DASH. J.L.D. and M.R.W. are Co-Investigators of the Precision Diagnosis of Acute Infectious Diseases study funded by

the CA Initiative to Advance Precision Medicine mentioned in the Discussion section. H.A.S. is the Program Manager of that study, and K.C.Z. is a clinical research coordinator working on that study.

## References

1. Grad YH, Lipsitch M. Epidemiologic data and pathogen genome sequences: a powerful synergy for public health. *Genome Biol* 2014;15:538.
2. Wilson M, Tyler KL. Emerging diagnostic and therapeutic tools for central nervous system infections. *JAMA Neurol* 2016;73:1389–1390.
3. Schubert RD, Wilson MR. A tale of two approaches: how metagenomics and proteomics are shaping the future of encephalitis diagnostics. *Curr Opin Neurol* 2015;28:283–287.
4. Holden P, Hess AD. Cache Valley virus, a previously undescribed mosquito-borne agent. *Science* 1959;130:1187–1188.
5. Nguyen NL, Zhao G, Hull R, et al. Cache valley virus in a patient diagnosed with aseptic meningitis. *J Clin Microbiol* 2013;51:1966–1969.
6. Campbell GL, Matczynski JD, Reisdorf ES, et al. Second human case of Cache Valley virus disease. *Emerg Infect Dis* 2006;12:854–856.
7. Sexton DJ, Rollin PE, Breitschwerdt EB, et al. Life-threatening Cache Valley virus infection. *N Engl J Med* 1997;336:547–549.
8. Nasreddine ZS, Phillips NA, Bedirian V, et al. The Montreal Cognitive Assessment, MoCA: a brief screening tool for mild cognitive impairment. *J Am Geriatr Soc* 2005;53:695–699.
9. Lee D, Das Gupta J, Gaughan C, et al. In-depth investigation of archival and prospectively collected samples reveals no evidence for XMRV infection in prostate cancer. *PLoS One* 2012;7:e44954.
10. Naccache SN, Greninger AL, Lee D, et al. The perils of pathogen discovery: origin of a novel parovirus-like hybrid genome traced to nucleic acid extraction spin columns. *J Virol* 2013;87:11966–11977.
11. Doan T, Wilson MR, Crawford ED, et al. Illuminating uveitis: metagenomic deep sequencing identifies common and rare pathogens. *Genome Med* 2016;8:90.
12. Wilson MR, Shanbhag NM, Reid MJ, et al. Diagnosing Balamuthia mandrillaris encephalitis with metagenomic deep sequencing. *Ann Neurol* 2015;78:722–730.
13. Wilson MR, Zimmermann LL, Crawford ED, et al. Acute West Nile virus meningoencephalitis diagnosed via metagenomic deep sequencing of cerebrospinal fluid in a renal transplant patient. *Am J Transplant* 2017;17:803–808.
14. Dobin A, Davis CA, Schlesinger F, et al. STAR: ultrafast universal RNA-seq aligner. *Bioinformatics* 2013;29:15–21.
15. Ruby JG, Bellare P, Derisi JL. PRICE: software for the targeted assembly of components of (Meta) genomic sequence data. *G3 (Bethesda)* 2013;3:865–880.
16. Fu L, Niu B, Zhu Z, et al. CD-HIT: accelerated for clustering the next-generation sequencing data. *Bioinformatics* 2012;28:3150–3152.
17. Ziv J, Lempel A. A universal algorithm for sequential data compression. *IEEE Trans Inf Theory* 1977;23:337–343.
18. Langmead B, Salzberg SL. Fast gapped-read alignment with Bowtie 2. *Nat Methods* 2012;9:357–359.
19. Wu TD, Nacu S. Fast and SNP-tolerant detection of complex variants and splicing in short reads. *Bioinformatics* 2010;26:873–881.
20. Zhao Y, Tang H, Ye Y. RAPSearch2: a fast and memory-efficient protein similarity search tool for next-generation sequencing data. *Bioinformatics* 2012;28:125–126.
21. Wang H, Nattanmai S, Kramer LD, et al. A duplex real-time reverse transcriptase polymerase chain reaction assay for the detection of California serogroup and Cache Valley viruses. *Diagn Microbiol Infect Dis* 2009;65:150–157.
22. Huang B, Firth C, Watterson D, et al. Genetic characterization of archived Bunyaviruses and their potential for emergence in Australia. *Emerg Infect Dis* 2016;22:833–840.
23. Rodrigues Hoffmann A, Welsh CJ, Wilcox Varner P, et al. Identification of the target cells and sequence of infection during experimental infection of ovine fetuses with Cache Valley virus. *J Virol* 2012;86:4793–4800.
24. Helbok R, Broessner G, Pfausler B, Schmutzhard E. Chronic meningitis. *J Neurol* 2009;256:168–175.
25. Tan CT, Goh KJ, Wong KT, et al. Relapsed and late-onset Nipah encephalitis. *Ann Neurol* 2002;51:703–708.
26. Wong SC, Ooi MH, Wong MN, et al. Late presentation of Nipah virus encephalitis and kinetics of the humoral immune response. *J Neurol Neurosurg Psychiatry* 2001;71:552–554.
27. Misbah SA, Spickett GP, Ryba PC, et al. Chronic enteroviral meningoencephalitis in agammaglobulinemia: case report and literature review. *J Clin Immunol* 1992;12:266–270.
28. Naccache SN, Peggs KS, Mattes FM, et al. Diagnosis of neuroinvasive astrovirus infection in an immunocompromised adult with encephalitis by unbiased next-generation sequencing. *Clin Infect Dis* 2015;60:919–923.
29. Quan PL, Wagner TA, Briese T, et al. Astrovirus encephalitis in boy with X-linked agammaglobulinemia. *Emerg Infect Dis* 2010;16:918–925.
30. Jun JB, Choi Y, Kim H, et al. BK polyomavirus encephalitis in a patient with thrombotic microangiopathy after an allogeneic hematopoietic stem cell transplant. *Transpl Infect Dis* 2016;18:950–953.
31. Ludlow M, Kortekaas J, Herden C, et al. Neurotropic virus infections as the cause of immediate and delayed neuropathology. *Acta Neuropathol* 2016;131:159–184.
32. Morfopoulou S, Mee ET, Connaughton SM, et al. Deep sequencing reveals persistence of cell-associated mumps vaccine virus in chronic encephalitis. *Acta Neuropathol* 2017;133:139–147.
33. Soldan SS, Gonzalez-Scarano F. The Bunyaviridae. *Handb Clin Neurol* 2014;123:449–463.
34. Soldan SS, Gonzalez-Scarano F. Emerging infectious diseases: the Bunyaviridae. *J Neurovirol* 2005;11:412–423.
35. Walters LL, Tirrell SJ, Shope RE. Seroepidemiology of California and Bunyamwera serogroup (Bunyaviridae) virus infections in native populations of Alaska. *Am J Trop Med Hyg* 1999;60:806–821.
36. Campbell GL, Reeves WC, Hardy JL, Eldridge BF. Seroepidemiology of California and Bunyamwera serogroup bunyavirus infections in humans in California. *Am J Epidemiol* 1992;136:308–319.
37. Kosoy O, Rabe I, Geissler A, et al. Serological survey for antibodies to mosquito-borne bunyaviruses among US National Park Service and US Forest Service employees. *Vector Borne Zoonotic Dis* 2016;16:191–198.
38. Calisher CH, Franci DB, Smith GC, et al. Distribution of Bunyamwera serogroup viruses in North America, 1956–1984. *Am J Trop Med Hyg* 1986;35:429–443.
39. Andreadis TG, Armstrong PM, Anderson JF, Main AJ. Spatial-temporal analysis of Cache Valley virus (Bunyaviridae: Orthobunyavirus) infection in anopheline and culicine mosquitoes (Diptera: Culicidae) in the northeastern United States, 1997–2012. *Vector Borne Zoonotic Dis* 2014;14:763–773.
40. Faria NR, Azevedo Rdo S, Kraemer MU, et al. Zika virus in the Americas: early epidemiological and genetic findings. *Science* 2016;352:345–349.
41. Faria NR, Rambaut A, Suchard MA, et al. HIV epidemiology. The early spread and epidemic ignition of HIV-1 in human populations. *Science* 2014;346:56–61.